



Cite this: *Org. Biomol. Chem.*, 2021, **19**, 677

## Acceptorless dehydrogenative condensation: synthesis of indoles and quinolines from diols and anilines†

Delia Bellezza, Ramón J. Zaragoza,  M. José Aurell,  Rafael Ballesteros  and Rafael Ballesteros-Garrido \*

The use of diols and anilines as reagents for the preparation of indoles represents a challenge in organic synthesis. By means of acceptorless dehydrogenative condensation, heterocycles, such as indoles, can be obtained. Herein we present an experimental and theoretical study for this purpose employing heterogeneous catalysts Pt/Al<sub>2</sub>O<sub>3</sub> and ZnO in combination with an acid catalyst (*p*-TSA) and NMP as solvent. Under our optimized conditions, the diol excess has been reduced down to 2 equivalents. This represents a major advance, and allows the use of other diols. 2,3-Butanediol or 1,2-cyclohexanediol has been employed affording 2,3-dimethyl indoles and tetrahydrocarbazoles. In addition, 1,3-propanediol has been employed to prepare quinolines or natural and synthetic julolidines.

Received 24th September 2020,  
Accepted 17th December 2020

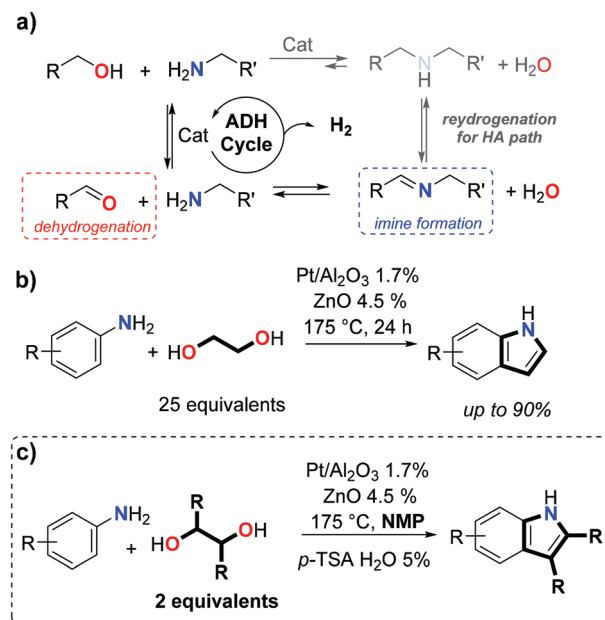
DOI: 10.1039/d0ob01964j

rsc.li/obc

### Introduction

Borrowing Hydrogen reactions (BH),<sup>1</sup> also known as Hydrogen Autotransfer reactions (HA),<sup>2</sup> have gained significant attention in the last decade. This type of reaction falls within the framework of green chemistry,<sup>3</sup> both for its high atomic efficiency and for the use of catalysis. In addition, only water is obtained as a side-product. The BH process is based on an alcohol dehydrogenation followed by imine formation as shown in Scheme 1(a). The hydrogen abstracted from the alcohols is then employed to form a secondary amine by rehydrogenation.<sup>2–5</sup> In all contributions reported on this reaction, homogeneous catalysts have been by far the most used.<sup>2</sup> These types of reaction are applied to many alcohols, but diols are particularly interesting. Diols can lead to single and/or double HA/BH reactions as reported by Williams<sup>4</sup> or even frustrated-HA/BH reactions (also named acceptorless dehydrogenative condensation (ADH), Scheme 1);<sup>6</sup> ADH may yield heterocycles such as pyrroles.<sup>7</sup> Interestingly, ethylene glycol has not been extensively employed compared to other diols. However, ethylene glycol can be used to prepare amino-alcohols<sup>8</sup> and, more importantly, indoles<sup>9</sup> (Scheme 1 middle). Madsen and collaborators published that other types of 1,2-diol can be used for indole synthesis. In their work, homogeneous ruthenium or iridium catalysts were employed with equimolar aniline/diol

amounts.<sup>10</sup> Heterogeneous catalysts for HA/BH or ADH have been less exploited.<sup>11</sup> As a general trend, an excess of alcohol is necessary for efficient ADH reactions.<sup>3</sup> In our previous studies, ethylene glycol was indeed used also as a solvent.<sup>8,9</sup> When the alcohol is accessible (economically), an excess may



**Scheme 1** (a) General ADH reaction mechanism. (b) Previous results with ethylene glycol and anilines. (c) Optimal conditions with two equivalents of diol.

University of Valencia, Av. Vicent Andrés Estellés, s/n. 46100, Burjassot, Valencia, Spain. E-mail: rafael.ballesteros-garrido@uv.es

† Electronic supplementary information (ESI) available. See DOI: 10.1039/d0ob01964j

be acceptable, as is the situation with ethanol, methanol, benzyl alcohol or ethylene glycol. When more complex alcohols are required, the excess appears as a major drawback for the methodology. However, complex diols do work on these systems, as can be concluded from the pioneering works of Watanabe,<sup>12</sup> where even 1,2-cyclohexanediol was employed for the preparation of tetrahydrocarbazoles. Herein we focus on optimizing the conditions for the formation of complex indoles through heterogeneous catalysis. Theoretical calculations have been carried out in order to establish a plausible reaction mechanism.

## Results and discussion

In our previous studies we found that a combination of Pt/Al<sub>2</sub>O<sub>3</sub> and ZnO was able to activate ethylene glycol.<sup>9</sup> Under these conditions, hydrogen was *in situ* released. Glycolaldehyde production triggered the indole formation cycle. The practical use of other 1,2-diols is not only based on their price, but also on their physical state (many of them are solid compounds and cannot act as solvent). Thus, a BH/HA compatible solvent was required.

### Reaction optimization

Trimethoxy aniline **1a** was chosen as the model aniline due to its performance in ADH reaction observed in our previous work.<sup>9</sup> With this compound different solvents were evaluated. NMP afforded the best results, and imino ketone **2a** (37%) and 37% indole **3a** were obtained. DMA, DMF and DMSO did not improve these results. Using diglyme, low yields were also obtained. The presence of **2a** was unexpected. In any of our previous results with ethylene glycol (as solvent), ketones or aldehydes were never observed; in contrast, morpholines, diamines or amino alcohols were common side products,<sup>8,9</sup> but not imino ketones. Indeed, by employing *o*-2,4-dimethylaniline (**1b**), amino ketones **2b** were obtained, and no trace of the corresponding indole was observed. *p*-TSA was introduced in the reaction expecting that this acid catalyst will help in intramolecular cyclization. It is worth noting that in the literature compound **2a** was directly obtained by the condensation of 3-hydroxybutan-2-one and **1a**.<sup>12,13</sup> A major difference with secondary alcohols under BH/HA cycles is that ketones are obtained instead of aldehydes (glycolaldehyde for ethylene glycol). Ketones appear to be less reactive towards the S<sub>E</sub>Ar reactions compared to aldehydes. Acids (both Lewis and Brønsted) are common catalysts for these reactions. When *p*-TSA was introduced in the reaction (5%), the yield increased to 99% for compound **3a**. With this new catalyst combination, solvents were screened again with a significant improvement of yields. NMP remained the most efficient (Fig. 1, bottom). In addition, the equivalent amount could be reduced down to 2 equivalents keeping the concentration at 0.8 M and the reaction time is no longer than 48 h (controlled by TLC).

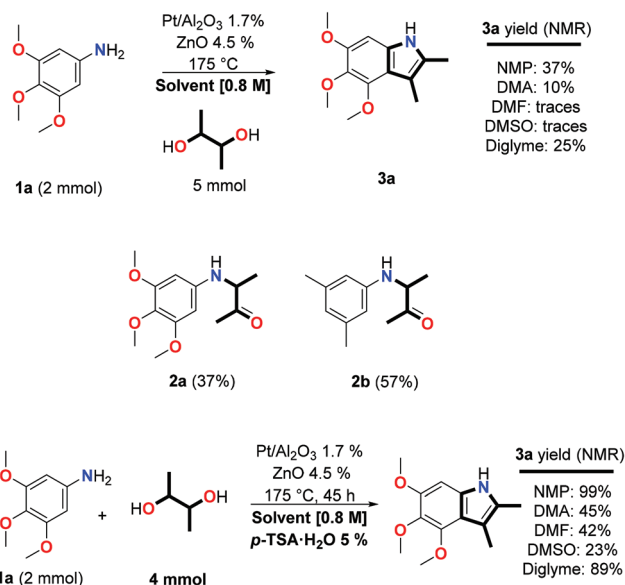


Fig. 1 Solvent screening and *p*-TSA results.

### 2,3-Butanediol

In Fig. 2, the aniline scope with 2,3-butanediol is presented. Substituted anilines **1a–c** afforded indoles **3a–c** with good yields except for compound **3c** (30%). However, no trace of amino ketone was observed. 1-Naphthyl amine (**1d**) afforded indole **3d** in 79% yield and aniline compound **3e** in 70% yield. 2,5-Dimethoxyaniline gave indole **3f** in 99% yield. Tetrahydroquinoline allowed the synthesis of tricyclic compound **3g** in an excellent yield of 86%. However, indoline did not afford indole formation. Instead, amino ketone **2d** was iso-

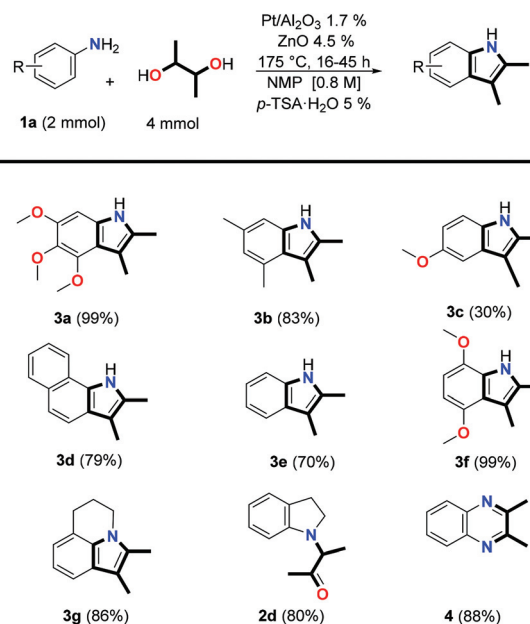


Fig. 2 Aniline scope with 2,3-butanediol.

lated in 80%. Structures with [5,5,6] condensed cycles are not commonly reported in the literature due to ring tension. The presence of amino ketone clearly points towards this explanation. 1,2-Diamino benzene afforded quinoxaline **4** (88%). The presence of compound **4** can also be related to the imino ketone intermediate (*vide infra*).

### Mechanism studies and theoretical calculations

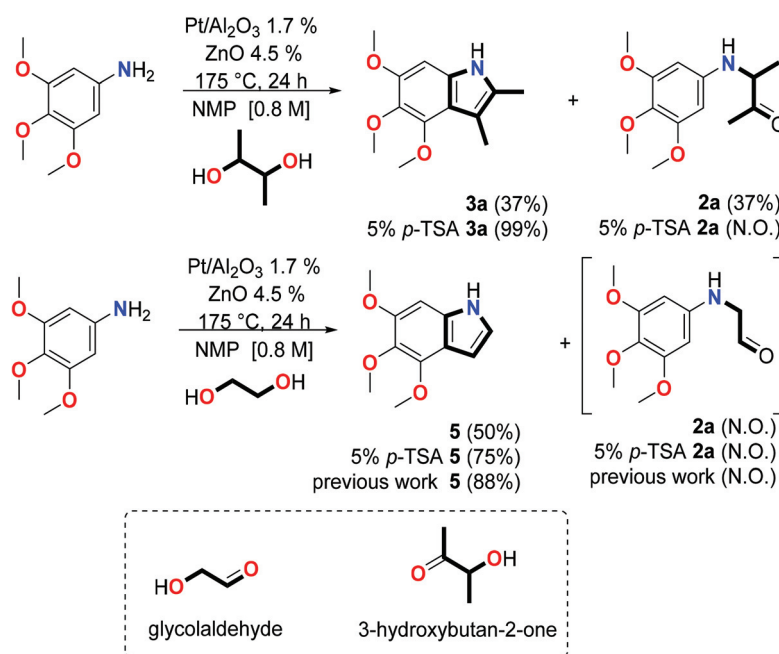
To shed light on the mechanism and understand the observed differences (the presence of amino ketones and the requirement of acid catalysis), DFT calculations (B3LYP-D3) and additional experiments were performed. It is important to note that this process starts with a single alcohol dehydrogenation and, after this step, imine formation occurs.

Scheme 2 shows the control reactions with 2,3-butanediol and ethylene glycol. On employing two equivalents of ethylene glycol (Pt/Al<sub>2</sub>O<sub>3</sub>, NMP, without an acid catalyst) compound **5** was obtained in 50% yield and 75% when *p*-TSA was used. This difference in performance is remarkable, because if ethylene glycol is used as solvent (6 mL) **5** can be obtained in 88% yield according to our previous studies.<sup>9</sup> Zhang and collaborators also observed this difference in their approach with a Ru-Xantphos catalyst.<sup>14</sup> In fact, under their conditions, ethylene glycol was not able to undergo indole formation with aniline. Consequently, dehydrogenation of ethylene glycol is more difficult to achieve compared to that of 2,3-butanediol. In Watanabe's original studies a similar behavior was reported,<sup>12</sup> and higher yields with 2,3-butanediol were obtained. However, the most surprising result of these reactions was the absence of aldehydes in the reaction medium. Without acid catalysis, amino ketones appear (Scheme 2 top); in the case of ethylene glycol, aldehydes have never been observed, either under these

conditions or in our previous studies. In addition, neither glycolaldehyde nor 3-hydroxybutan-2-one (dehydrogenation products, Scheme 2 bottom) is observed in the reaction mixture, and this is in coherence with a fast initial imine formation. Fig. 3 presents the overall mechanism proposed for this reaction.

As can be seen in Fig. 3 (see also Table S4†), starting from the imine (**1a**), an initial tautomeric equilibrium yields the imino ketone. This equilibrium is mediated by a water molecule that acts as a catalyst being present in **TS1a** and **TS2a** with 41.2 and 34.8 kcal mol<sup>-1</sup> barriers, respectively. The overall energetic balance makes the final ketone more stable than any of the intermediates. Water is present as a side product from the imine formation and also because ZnO is used as water suspension.

These calculations agree with the experimental observations as only amino ketones are observed. Intramolecular cyclisation is the following step. As can be noted, a prochiral carbon is present in ketone **IN2a**. Thus two different attacks can take place, *re* (Fig. 3 middle, red path) or *si* (blue path) attacks (both mediated by a water molecule again), and they have similar TS energies (**TS3a1** and **TS3a2**: 36.9 and 37.5 kcal mol<sup>-1</sup>). The final products **IN3a1** and **IN3a2** are diastereoisomers (both being racemic due to the initial racemic state of 3-hydroxybutan-2-one). At this stage, water elimination is required to create aromaticity in the 5-membered ring. However, only *syn*-elimination is possible, owing to catalysis by the water molecule in a cyclic **TS4a1**. Anti-elimination cannot occur, under an accessible energy level, due to the trans arrangement of the alcohol and hydrogen group, even with a water molecule. For a more general comparison, similar calculations were performed with ethylene glycol (see the ESI, Fig. S15–S17† at the B3LYP level).



Scheme 2 Ethylene glycol versus 2,3-butanediol (N.O. = not observed).

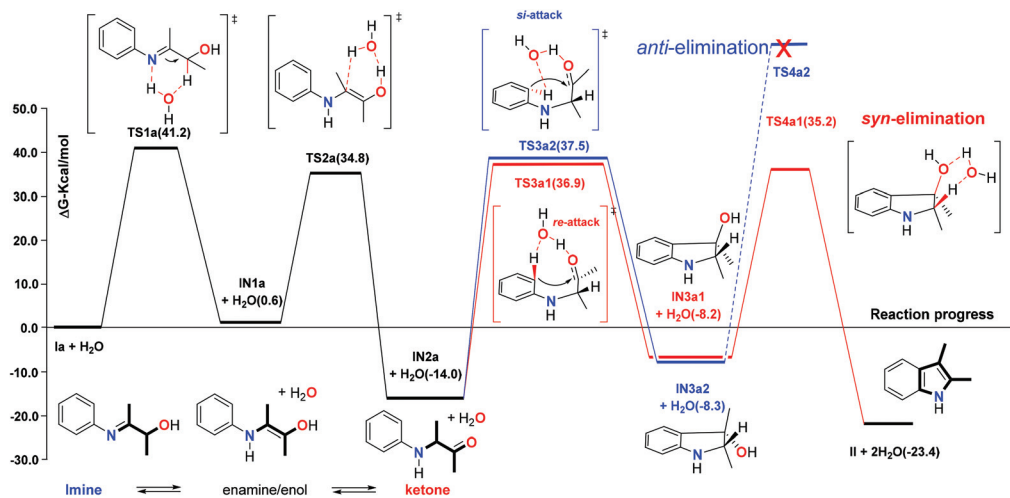


Fig. 3 Mechanism for the transformation of the imine Ia into indole II catalyzed with H<sub>2</sub>O at the B3LYP-D3 level.

Two significant differences can be found. First, the transition state for the intramolecular cyclization is lower, 3.4 kcal mol<sup>-1</sup>, and this is in coherence with the experimental observation: the absence of aldehydes and the spontaneous conversion to indoles upon oxidation.<sup>8,9</sup> The second relevant difference is the absence of *re* and *si* faces, as a consequence and a hydrogen atom (of the CH<sub>2</sub>) is always accessible to eliminate a water molecule.

Next, the system was modeled with acid catalysis (Fig. 4). Indeed, major changes occur under these conditions. First, tautomeric equilibrium is affected, reducing TS barriers significantly (Ts1b).

Under the acidic conditions of *p*-TSA (pK<sub>a</sub> = -2.8) the imine Ia is initially protonated providing Ib (Fig. 4). The positive charge is delocalized between the N and C of the imine (in fact between the H on the N and the C-2 of the imine see Fig. S3†). The mechanism by which Ib is transformed in indole II differs dramatically from the one described above without catalysis. Isomerization of protonated imine Ib in the ketone IN2b1

takes place in a single stage (note that without acid catalysis two stages are required; TS1a and TS2a Fig. 3), through TS1b with an energy barrier (ΔG) of 25.5 kcal mol<sup>-1</sup>. In TS1b, transposition of H over C-1 to C-2 occurs through a three-membered cyclic state. This transposition is favored by the positive partial charge on C-2 (see the ESI†). The H<sub>2</sub>O acts by stabilizing the TS by forming two hydrogen bonds with the protons over the N and O of the hydroxyl.

The nucleophilic attack of the aromatic ring on the carbonyl of the ketone IN2b1 is preceded by the initial transfer of the proton to the carbonyl to give IN2b2. The presence of the H<sub>2</sub>O molecule facilitates the transfer of the hydrogen atom. This enhances the electrophilic character and facilitates the attack of the aromatic ring, being indeed a classic acid catalyzed S<sub>E</sub>Ar.

In this case, again the intramolecular S<sub>E</sub>Ar can proceed through *re*-attack and *si*-attack on both sides of the ketone carbonyl. The *re*-attack gives rise to IN3b1 through TS3b1, with an energy barrier from IN2b1 of 35.1 kcal mol<sup>-1</sup> (blue path).

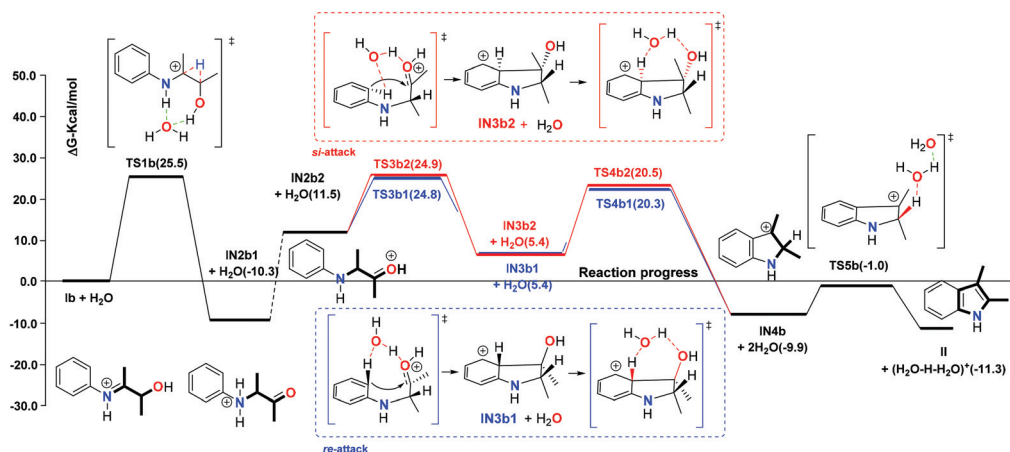


Fig. 4 Mechanism for the transformation of the imine Ia into indole II catalyzed with H<sub>2</sub>O and *p*-TSA at the B3LYP-D3 level.

Similarly, the *si*-attack (red path) leads to **IN3b2** through **TS3b2** ( $\Delta G = 35.2 \text{ kcal mol}^{-1}$  from **IN2b1**). In both intermediates **IN3b1/IN3b2** there has been no abstraction of H over the ring and therefore its rearomatization. This situation differs from that observed for the corresponding **IN3a1/IN3a2**, of the mechanism without acid catalysis, where the simultaneous rearomatization of the benzene ring occurs.

Both cationic alcohols **IN3b1/IN3b2** evolve through **TS4b1/TS4b2** to the same **IN4b** carbocation. In **TS4b1/TS4b2** the abstraction of the H occurs with rearomatization of the benzene ring and the simultaneous expulsion of the hydroxyl. In this case there is no geometric restriction observed for **TS4a1/TS4a2** (without acid catalysis, Fig. 3), and both the paths through *re*-attack and *si*-attack can lead to the final product. The energy barriers from **IN3b1/IN3b2** are 14.9/15.2  $\text{kcal mol}^{-1}$  for **TS4b1/TS4b1**, respectively. Finally, aromatization by elimination of H in **IN4b** leads to indole **II** through **TS5b** ( $\Delta G = 8.9 \text{ kcal mol}^{-1}$  from **IN4b**).

In addition, it is noteworthy that under acidic conditions the energy of the whole process is clearly inferior (around 15  $\text{kcal mol}^{-1}$ ). This is in agreement with experimental observations. Although the calculated energy barriers are too high, the inclusion of an additional molecule in the vicinity of the water molecule that acts as a catalyst lowers these barriers (see Fig. S18–S19 in the ESI†).

### 1,2-Cyclohexanediol and 1,3-propanediol

In order to expand the methodology, 1,2-cyclohexanediol was employed for the preparation of tetrahydrocarbazoles.

Tetrahydrocarbazoles are relevant compounds in medicinal chemistry; however, their preparation requires hydrazine derivatives. Fischer indole synthesis is the easiest access to these structures. Looking in detail in the literature, Watanabe also reported on this transformation with moderate yields.<sup>12</sup> Madsen also corroborated this approach.<sup>10</sup> Importantly, 1,2-cyclohexanediol has been employed for the preparation of piperazines.<sup>15</sup> Fig. 5 shows the aniline scope with this diol. Two equivalents of diol were employed under identical conditions to those employed for 2,3-butanediol. Trimethoxy derivative **7a** was prepared in excellent yield (99%). The corresponding compounds **7b–f** were obtained in moderate yields (from 33% to 45%). The tetracyclic compound **7g** was obtained in good yield (67%). When 1,2-diamino benzene (**1i**) was used as a reagent, the corresponding quinoxaline **8** was isolated in 23% yield. Compound **8** and compound **4** (2,3-dimethyl-quinoxaline from Fig. 2) provide clear evidence of the presence of amino ketones (Scheme 3). In the literature there are many examples of this reaction with 1,2-diols and 1,2-diaminobenzene (**1i**).<sup>16–20</sup>

Additional reactions were performed with asymmetric 1,2-propanediol. Under these conditions, compounds **9a** and **9b** were obtained as a mixture with good yield (79%, Scheme 3; bottom). An 84/16 ratio of the 2-methyl indole **9a** and the 3-methyl indole **9b** was observed. The presence of both isomers can be explained either by initial oxidation of different alcohols or the internal tautomeric equilibrium.<sup>21</sup>

Finally, 1,3-propanediol was employed. Watanabe reported an original access towards quinolines with the homogeneous

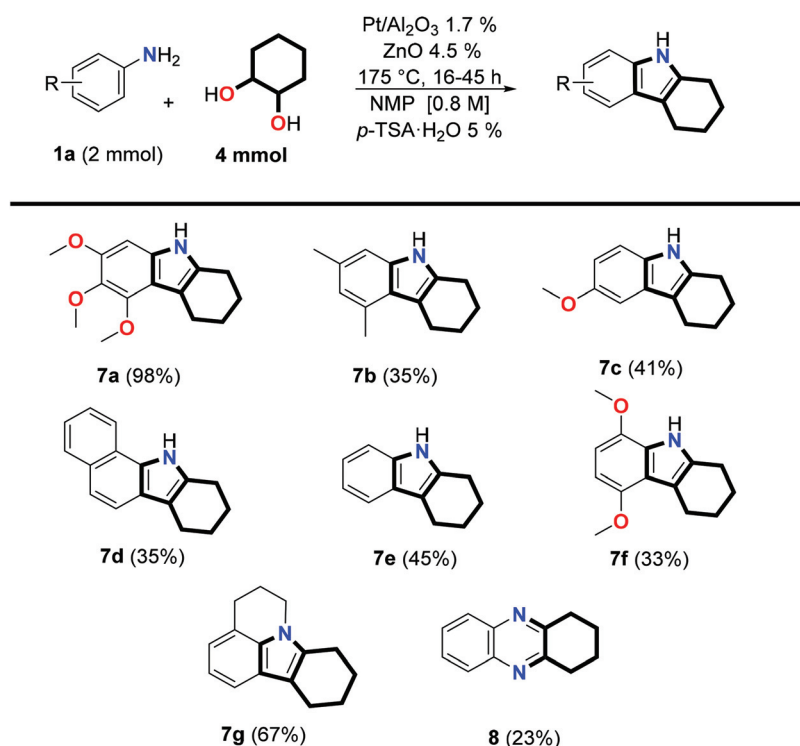
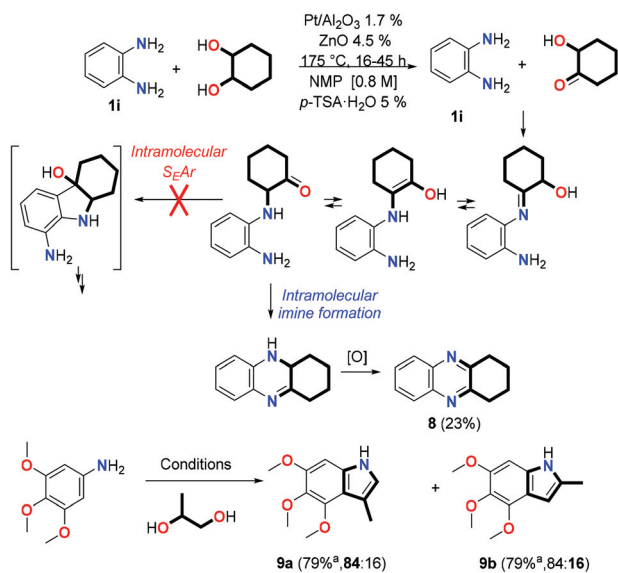
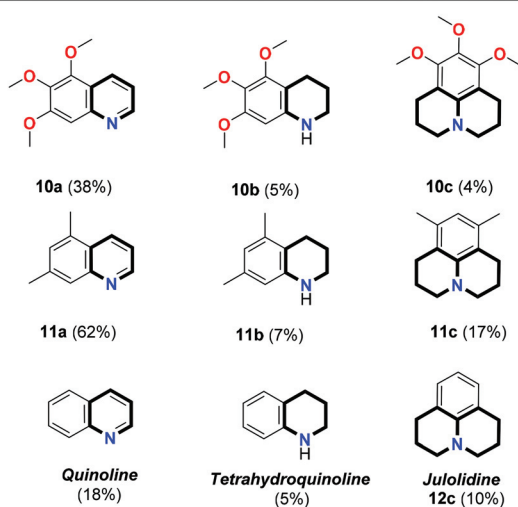
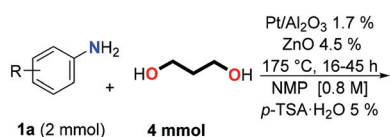


Fig. 5 Aniline scope with 1,2-cyclohexanediol.



**Scheme 3** Mechanism rationale for quinoxaline **8** formation and 1,2-propanediol reaction. (a) Yield given for the isomeric mixture.



**Fig. 6** Aniline scope with 1,3-propanediol.

Ru(II) catalyst employing 1,3-propanediol and anilines.<sup>22</sup> Madsen combined a ruthenium catalyst with a Lewis acid also for such an approach.<sup>23</sup> In our previous studies with Pd/C and ZnO (water/diol excess) a combination of  $\lambda$ -amino alcohols and quinolines was observed with low yields.<sup>24</sup>

Fig. 6 shows the results of this reaction. As can be seen, a combination of products was always obtained. Indeed, quinolines were the major products (compounds **10a**, **11a** and quinoline) obtained in moderate yields (38%, 62% and 18%,

respectively). Tetrahydroquinolines **10b**, **11b** and tetrahydroquinoline appeared as trace products. Interestingly, julolidines were also isolated (compounds **10c**, **11c** and **12c**) in low yields. Bruenau reported on the synthesis of these compounds under similar conditions with an iridium/BINAP catalyst.<sup>25</sup> These results clearly indicate that more complex structures can be obtained with distant alcohols, and although selectivity is a major issue, even tricyclic compounds as natural and interesting products such as julolidines can be synthesized.

## Conclusion

Herein, 2,3-dimethylindole and tetrahydrocarbazole synthesis is reported employing anilines and 1,2-diols at a 1:2 molar ratio. Pt/Al<sub>2</sub>O<sub>3</sub>, ZnO and *p*-TSA catalyze this transformation using NMP as solvent (0.8 M). DFT calculations and mechanism studies have unveiled the relevance of *p*-TSA; indeed, a carbocation has been found as a key intermediate in the mechanism. In addition, by employing 1,3-propanediol as a reagent, quinolines and julolidines have been prepared.

## Experimental section

### Computational methods

All calculations were carried out with the Gaussian 09 suite of programs.<sup>26</sup> Initially, density functional theory<sup>27</sup> calculations (DFT) have been carried out using the B3LYP<sup>28</sup> exchange–correlation functionals, together with the standard 6-31G(d) basis set, in the gas phase.<sup>29</sup> The stationary points were characterized by frequency computations in order to verify that TSs have one and only one imaginary frequency. The intrinsic reaction coordinate (IRC) paths<sup>30</sup> were traced in order to check the energy profiles connecting each TS to the two associated minima of the proposed mechanisms using the second order González–Schlegel integration method.<sup>31</sup> Subsequently, the inclusion of solvent effects has been considered by using a relatively simple self-consistent reaction field (SCRF) method<sup>32</sup> based on the polarizable continuum model (PCM) of Tomasi's group.<sup>33</sup> As solvents we have used *N,N*-dimethylacetamide (similar to 1-methylpyrrolidin-2-one used experimentally). The values of enthalpies, entropies and free energies in *N,N*-dimethylacetamide were calculated with the standard statistical thermodynamics at 423.15 K.<sup>29</sup> Due to the presence of hydrogen bonds, and in order to obtain more precise energy results, all species have been recalculated by single-point energy calculation at the B3LYP-D3 level.

### General procedure

Aniline (1 equiv., 2 mmol) (THQ or indoline), 1.7% of Pt/Al<sub>2</sub>O<sub>3</sub> (132.5 mg), 4.5% of ZnO nanoparticles (21.5  $\mu$ L) (<100 nm particle size (DLS), <0 nm average particle size (APS), 20 wt% in H<sub>2</sub>O), 5% of *p*-TSA H<sub>2</sub>O (19 mg), diol (2 equiv., 4 mmol), and 2.5 mL of NMP were mixed manually inside a 50 mL quick-thread glass reaction tube. The tube was sealed with an Easy-

On PTFE cap and put into a Carousel 12 Plus reaction station at 175 °C for 24–48 h (controlled by TLC). The reaction mixture was cooled to room temperature, and it needed to be opened carefully to depressurize the tube. After that, 15 mL of ethyl acetate was added, and the crude product was filtered through a 0.45 µm PTFE filter. The reaction mixture was washed with distilled water (3 × 10 mL), and the organic layer was dried with Na<sub>2</sub>SO<sub>4</sub>, filtered, and concentrated to afford the reaction crude product that was examined by <sup>1</sup>H NMR. The crude reaction product was purified by column chromatography using Merck 60 (0.040–0.063 mm) silica gel and a mixture of hexane (5)/ethyl acetate (1) as the eluent.

## Conflicts of interest

The authors state that there are no conflicts to declare.

## Acknowledgements

This work was financially supported by the Ministerio de Economía, Industria y Competitividad (CONSOLIDER CTQ2017-90852-REDC), Generalitat Valenciana (Prometeo/2015/002) and the Universitat de València (Spain) (UV-INV\_AE19-1205699).

## Notes and references

- 1 A. J. A. Watson and J. M. J. Williams, *Science*, 2010, **329**, 635.
- 2 G. Guillena, D. J. Ramon and M. Yus, *Chem. Rev.*, 2010, **110**, 1611.
- 3 C.-J. Li and B. M. Trost, *Proc. Natl. Acad. Sci. U. S. A.*, 2008, **105**, 13197.
- 4 M. H. S. A. Hamid, C. L. Allen, G. W. Lamb, A. C. Maxwell, H. C. Maytum, A. J. A. Watson and J. M. J. Williams, *J. Am. Chem. Soc.*, 2009, **131**, 1766.
- 5 M. H. S. A. Hamid, P. A. Slatford and J. M. J. Williams, *Adv. Synth. Catal.*, 2007, **349**, 1555.
- 6 C. Gunanathan and D. Milstein, *Science*, 2013, **314**, 1229712.
- 7 S. Michlik and R. Kempe, *Nat. Chem.*, 2013, **5**, 140.
- 8 P. J. Llabres-Campaner, R. Ballesteros-Garrido, R. Ballesteros and B. Abarca, *Tetrahedron*, 2017, **73**, 5552.
- 9 P. J. Llabres-Campaner, R. Ballesteros-Garrido, R. Ballesteros and B. Abarca, *J. Org. Chem.*, 2018, **83**, 521.
- 10 M. Tursky, L. L. R. Lorentz-Petersen, L. B. Olsen and R. Madsen, *Org. Biomol. Chem.*, 2010, **8**, 5576.
- 11 K. Shimizu, *Catal. Sci. Technol.*, 2015, **5**, 1412.
- 12 Y. Tsuji, K. T. Huh and Y. Watanabe, *J. Org. Chem.*, 1987, **52**, 1673.
- 13 A. Fuerstner, M. Alcarazo, V. Cesar and C. Lehmann, *Chem. Commun.*, 2006, **20**, 2176.
- 14 M. Zhang, F. Xie, X. T. Wang, F. Yan, T. Wang, M. Chen and Y. Ding, *RSC Adv.*, 2013, **3**, 6022.
- 15 A. Corma, T. Ródenas and M. J. Sabater, *Chem. – Eur. J.*, 2010, **16**, 254.
- 16 K. Chakrabarti, M. Maji and S. Kundu, *Green Chem.*, 2019, **21**, 1999.
- 17 P. Yang, C. Zhang, W.-C. Gao, Y. Mas, X. Wang, L. Zhang, J. Yue and B. Tang, *Chem. Commun.*, 2019, **55**, 7844.
- 18 M. J. Climent, A. Corma, J. C. Hernandez, A. B. Hungria, S. Iborra and S. Martínez-Silvestre, *J. Catal.*, 2012, **292**, 118.
- 19 F. Xie, M. Zhang, H. Jiang, M. Chen, L. Wan, A. Zheng and X. Jian, *Green Chem.*, 2015, **17**, 279.
- 20 M. Mastalir, M. Glatz, E. Pittenauer, G. Allmaier and K. Kirchner, *Org. Lett.*, 2019, **21**, 1116.
- 21 L. M. Azofra, M. M. Quesada-Moreno, I. Alkorta, J. R. Avilés-Moreno, J. Elguero and J. J. López-González, *ChemPhysChem*, 2015, **16**, 2226.
- 22 Y. Tsuji, H. Nishimura, K.-T. Huh and Y. Watanabe, *J. Organomet. Chem.*, 1985, **283**, c44.
- 23 R. N. Monrad and R. Madsen, *Org. Biomol. Chem.*, 2011, **9**, 610.
- 24 P. J. Llabres-Campaner, P. Woodbridge-Ortega, R. Ballesteros-Garrido, R. Ballesteros and B. Abarca, *Tetrahedron Lett.*, 2017, **58**, 4880.
- 25 A. Labeled, F. Jiang, I. Labeled, A. Lator, M. Peters, M. Achard, A. Kabouche, Z. Kabouche, G. V. M. Sharma and C. Bruneau, *ChemCatChem*, 2015, **7**, 7090.
- 26 M. J. Frisch, *et al.*, *Gaussian 09, Revision A.02*, Gaussian, Inc., Wallingford, CT, 2009.
- 27 (a) R. G. Parr and W. Yang, in *Density Functional Theory of Atoms and Molecules*, Oxford University Press, New York, 1989; (b) T. Ziegler, *Chem. Rev.*, 1991, **91**, 651.
- 28 (a) A. D. Becke, *J. Chem. Phys.*, 1993, **98**, 5648; (b) C. Lee, W. Yang and R. G. Parr, *Phys. Rev. B: Condens. Matter Mater. Phys.*, 1988, **37**, 785.
- 29 W. J. Hehre, L. Radom, P. von R. Schleyer and J. A. People, in *Ab initio Molecular Orbital Theory*, Wiley, New York, 1986.
- 30 K. Fukui, *J. Phys. Chem.*, 1970, **74**, 4161.
- 31 (a) C. González and H. B. Schlegel, *J. Phys. Chem.*, 1990, **94**, 5523; (b) C. González and H. B. Schlegel, *J. Chem. Phys.*, 1991, **95**, 5853.
- 32 (a) J. Tomasi and M. Persico, *Chem. Rev.*, 1994, **94**, 2027; (b) B. Y. Simkin and I. Sheikhet, in *Quantum Chemical and Statistical Theory of Solutions-A Computational Approach*, Ellis Horwood, London, 1995.
- 33 (a) E. Cancès, B. Mennucci and J. Tomasi, *J. Chem. Phys.*, 1997, **107**, 3032; (b) M. Cossi, V. Barone, R. Cammi and J. Tomasi, *Chem. Phys. Lett.*, 1996, **255**, 327; (c) V. Barone, M. Cossi and J. Tomasi, *J. Comput. Chem.*, 1998, **19**, 404.